Spectrum of short-wavelength magnons in a two-dimensional quantum Heisenberg antiferromagnet on a square lattice: third-order expansion in 1/*S*

2010 J. Phys.: Condens. Matter 22 216003

(http://iopscience.iop.org/0953-8984/22/21/216003)

J. Phys.: Condens. Matter **22** (2010) 216003 (7pp) doi:10.1088/0953-8984/22/21/216003

Spectrum of short-wavelength magnons in a two-dimensional quantum Heisenberg antiferromagnet on a square lattice: third-order expansion in $1/S$

A V Syromyatnikov

Petersburg Nuclear Physics Institute, Gatchina, St Petersburg 188300, Russia
and
Department of Physics, St Petersburg State University, Oulianovskaya 1, Petrodvorets, St Petersburg 198504, Russia

E-mail: syromyat@thd.pnpi.spb.ru

Received 26 January 2010, in final form 13 April 2010
Published 30 April 2010
Online at stacks.iop.org/JPhysCM/22/216003

Abstract
The spectrum of short-wavelength magnons in a two-dimensional quantum Heisenberg antiferromagnet on a square lattice is calculated to the third order in a $1/S$ expansion. It is shown that a $1/S$ series for $S = 1/2$ converges quickly in the whole Brillouin zone except in the neighborhood of the point $\mathbf{k} = (\pi, 0)$, at which absolute values of the third-and the second-order $1/S$-corrections are approximately equal to each other. It is shown that the third-order corrections make deeper the roton-like local minimum at $\mathbf{k} = (\pi, 0)$, improving the agreement with recent experiments and numerical results in the neighborhood of this point. It is suggested that the $1/S$ series converges slowly near $\mathbf{k} = (\pi, 0)$ also for $S = 1$ although the spectrum renormalization would be small in this case due to the very small values of high-order $1/S$ corrections.

1. Introduction

A spin-$\frac{1}{2}$ two-dimensional (2D) Heisenberg antiferromagnet (AF) on a square lattice has been one of the most attractive theoretical objects in the last two decades because this model describes parent compounds of high-T_c superconducting cuprates [1]. A number of theoretical approaches have been proposed to describe the spectrum of long-wavelength elementary excitations (magnons) in a quantum square 2D AF the results of which agree well with each other and describe quantitatively existing experimental data [1–3]. Meantime there are some surprising recent experimental and numerical findings, indicating that the standard theoretical approaches do not work for short-wavelength magnons for $S \sim 1$.

Thus, a roton-like local minimum was observed at small T in the spin-wave spectrum $\epsilon_{\mathbf{k}}$ at $\mathbf{k} = (\pi, 0)$ in a number of recent experiments on square spin-$\frac{1}{2}$ 2D AFs [4, 5, 3, 6]. In particular, the magnon energy at $\mathbf{k} = (\pi, 0)$ appears to be 7(1)% smaller than that at $\mathbf{k} = (\pi/2, \pi/2)$ in $Cu(DCOO)_2{\cdot}4D_2O$ [3]. This local minimum is a purely quantum effect as the classical spectrum of a 2D AF is flat along the magnetic Brillouin zone (BZ) boundary connecting points $(\pi, 0)$ and $(0, \pi)$ (see inset in figure 1). The spectrum near the point $\mathbf{k} = (\pi, 0)$ is not reproduced quantitatively within the second order in the $1/S$ expansion [7, 8] and phase flux resonating valence bond techniques [9]. In the former case the second-order corrections lead to a very small difference of 1.4% between $\epsilon^{(2)}_{(\pi,0)} \approx 2.358\,58$ and $\epsilon^{(2)}_{(\pi/2,\pi/2)} \approx 2.391\,99$ whereas in the last case this difference is too large. At the same time numerical computations using a series expansion around the Ising limit [10] and quantum Monte Carlo [11] describe the roton-like minimum satisfactorily, leading to values $\epsilon^{(\text{series})}_{(\pi,0)} \approx 2.18(1)$, $\epsilon^{(\text{series})}_{(\pi/2,\pi/2)} \approx 2.385(1)$ and $\epsilon^{(\text{MC})}_{(\pi,0)} \approx 2.16$, $\epsilon^{(\text{MC})}_{(\pi/2,\pi/2)} \approx 2.39$, respectively. The origin of the local minimum has not been clarified yet. It is considered to be a signature of the spins' entanglement on neighboring sites [3].

Existence of such a strong deviation of the spectrum near $\mathbf{k} = (\pi, 0)$ from the result obtained in the second order in $1/S$ is quite surprising because the second-order corrections

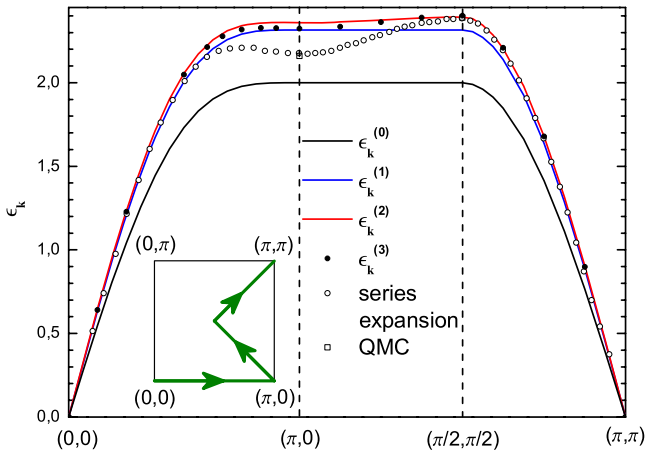

Figure 1. Spin-wave spectrum of a spin-$\frac{1}{2}$ AF along high-symmetry paths of the BZ shown in the inset. Here $\epsilon_{\mathbf{k}}^{(i)}$ indicates the spectrum calculated within the ith order in $1/S$ so that $i = 0$ corresponds to the classical spectrum (10). Results of the series expansion around the Ising limit and quantum Monte Carlo (QMC) computation (available only for $\mathbf{k} = (\pi, 0)$ and $(\pi/2, \pi/2)$) are also shown which were taken from [10] and [11], respectively. The former results describe quantitatively the spectrum observed experimentally [3] in $Cu(DCOO)_2{\cdot}4D_2O$.

(This figure is in colour only in the electronic version)

are much smaller than the first-order ones in the whole BZ even for $S = 1/2$ (see [7] and below) and one could expect a small contribution from high-order terms. Moreover, it is well known that the $1/S$ series for staggered magnetization, transverse susceptibility, ground state energy, and spin-wave stiffness of a 2D AF calculated up to the third order in $1/S$ converges surprisingly fast even for $S \sim 1$ despite the absence of a small parameter in the theory [1, 12–14, 8, 15]. As a result the quantitative agreement is very good between the $1/S$ expansion, numerical results, and experiments. It should be stressed that quantum renormalization of these quantities is considerable for $S \sim 1$. For instance, quantum fluctuations reduce the staggered magnetization in spin-$\frac{1}{2}$ 2D AF from its bare value of 0.5 to about 0.3. Meantime this renormalization is described quantitatively by the first few terms of the $1/S$ series.

We present in this present paper the results of a spectrum $\epsilon_{\mathbf{k}}^{(3)}$ calculation to the third order in $1/S$ and demonstrate that the $1/S$ series converges very fast in the whole BZ except in the vicinity of the point $\mathbf{k} = (\pi, 0)$ in the case of $S \sim 1$. In particular, we show that absolute values of the third-order corrections to the spectrum at $\mathbf{k} = (\pi, 0)$ are approximately equal to and only 2.5 times smaller than the second-order ones for $S = 1/2$ and $S = 1$, respectively. Thus, our results demonstrate that, unlike other quantities, quantum renormalization of the spectrum near $\mathbf{k} = (\pi, 0)$ for $S \sim 1$ is described by a slowly converging $1/S$ series. We find that the excitation energy in a spin-$\frac{1}{2}$ 2D AF $\epsilon_{(\pi,0)}^{(3)} \approx 2.3241(2)$ is 3.2% smaller than $\epsilon_{(\pi/2,\pi/2)}^{(3)} \approx 2.4007(2)$ which improves (but still does not make perfect) the agreement with the recent experiments and numerical results (see figure 1). We suggest that, despite the slow convergence of the $1/S$ series, the overall renormalization of the spectrum for $S = 1$ might be small due to very small values of high-order $1/S$ corrections.

The rest of this paper is organized as follows. We present the basic transformation of the Hamiltonian and describe the technique in section 2. Spectrum renormalization is discussed in section 3. Section 4 contains our conclusion. Expressions for self-energy parts in the third order in $1/S$ are presented in an appendix.

2. Basic transformations and techniques

The Hamiltonian of the Heisenberg AF on a square lattice with interaction between only nearest neighbor spins has the form

$$\mathcal{H} = \frac{J}{2} \sum_{\langle i,j \rangle} \mathbf{S}_i \mathbf{S}_j. \tag{1}$$

We put exchange constant $J = 1$ in all particular numerical calculations performed in the present paper. It is convenient to represent spins components in the local coordinate frame using the Dyson–Maleev transformation in the following way:

$$\mathbf{S}_j = S_j^x \hat{x} + (S_j^y \hat{y} + S_j^z \hat{z}) e^{i\mathbf{k}_0 \mathbf{R}_j}, \tag{2}$$

$$S_j^x = \sqrt{\frac{S}{2}} \left(a_j + a_j^\dagger - \frac{a_j^\dagger a_j^2}{2S} \right),$$

$$S_j^y = -i\sqrt{\frac{S}{2}} \left(a_j - a_j^\dagger - \frac{a_j^\dagger a_j^2}{2S} \right), \tag{3}$$

$$S_j^z = S - a_j^\dagger a_j,$$

where $\hat{x}$, $\hat{y}$, and $\hat{z}$ are unit vectors along corresponding axes and $\mathbf{k}_0 = (\pi, \pi)$ is the AF vector. As a result one finds that the Hamiltonian (1) acquires the form $\mathcal{H} = E_0 + \sum_{m=1}^{6} \mathcal{H}_m$, where E_0 is the classical value of the ground state energy and $\mathcal{H}_m$ denote terms containing products of m operators a and $a^\dagger$. $\mathcal{H}_m = 0$ for odd m and one has for even m

$$\mathcal{H}_2 = \sum_{\mathbf{k}} \left[E_{\mathbf{k}} a_{\mathbf{k}}^\dagger a_{\mathbf{k}} + \frac{B_{\mathbf{k}}}{2} (a_{\mathbf{k}} a_{-\mathbf{k}} + a_{\mathbf{k}}^\dagger a_{-\mathbf{k}}^\dagger) \right], \tag{4}$$

$$\mathcal{H}_4 = -\frac{1}{2N} \sum_{\mathbf{k}_{1,2,3,4}} a_{-1}^\dagger (J_{2+3} a_{-2}^\dagger + J_3 a_2) a_3 a_4, \tag{5}$$

$$\mathcal{H}_6 = \frac{1}{8SN^2} \sum_{\mathbf{k}_{1,2,3,4,5,6}} J_{1+3+4} a_{-1}^\dagger a_{-2}^\dagger a_3 a_4 a_5 a_6, \tag{6}$$

where $J_{\mathbf{k}} = 2(\cos k_x + \cos k_z)$, $E_{\mathbf{k}} = SJ_0$, $B_{\mathbf{k}} = SJ_{\mathbf{k}}$, N is the number of spins in the lattice, we drop index $\mathbf{k}$ in equations (5) and (6) and the momentum conservation laws $\sum_{i=1}^{4} \mathbf{k}_i = \mathbf{0}$ and $\sum_{i=1}^{6} \mathbf{k}_i = \mathbf{0}$ are implied in equations (5) and (6), respectively.

Introducing Green's functions $G(k) = \langle a_{\mathbf{k}}, a_{\mathbf{k}}^\dagger \rangle_\omega$, $F(k) = \langle a_{\mathbf{k}}, a_{-\mathbf{k}} \rangle_\omega$, $\bar{G}(k) = \langle a_{-\mathbf{k}}^\dagger, a_{-\mathbf{k}} \rangle_\omega$, and $F^\dagger(k) = \langle a_{-\mathbf{k}}^\dagger, a_{\mathbf{k}}^\dagger \rangle_\omega$, where $k = (\omega, \mathbf{k})$, we have two sets of Dyson equations for them one of which has the following form:

$$G(k) = G^{(0)}(k) + G^{(0)}(k)\bar{\Sigma}(k)G(k) + G^{(0)}(k)[B_{\mathbf{k}} + \Pi(k)]F^\dagger(k), \tag{7}$$

$$F^\dagger(k) = \bar{G}^{(0)}(k)\Sigma(k)F^\dagger(k) + \bar{G}^{(0)}(k)[B_{\mathbf{k}} + \Pi^\dagger(k)]G(k),$$

where $G^{(0)}(k) = (\omega - E_{\mathbf{k}})^{-1}$ is the bare Green's function and $\Sigma(k)$, $\bar{\Sigma}(k)$, $\Pi(k)$, and $\Pi^{\dagger}(k)$ are self-energy parts. By solving equations (7) and similar sets of equations for $\bar{G}(k)$ and $F(k)$ one obtains

$$G(k) = \frac{\omega + E_{\mathbf{k}} + \Sigma(k)}{\mathcal{D}(k)},$$

$$\bar{G}(k) = \frac{-\omega + E_{\mathbf{k}} + \bar{\Sigma}(k)}{\mathcal{D}(k)}, \tag{8}$$

$$F(k) = -\frac{B_{\mathbf{k}} + \Pi(k)}{\mathcal{D}(k)}, \qquad F^{\dagger}(k) = -\frac{B_{\mathbf{k}} + \Pi^{\dagger}(k)}{\mathcal{D}(k)},$$

where

$$\mathcal{D}(k) = \omega^2 - (\epsilon_{\mathbf{k}}^{(0)})^2 - \Omega(k), \tag{9}$$

$$\epsilon_{\mathbf{k}}^{(0)} = \sqrt{E_{\mathbf{k}}^2 - B_{\mathbf{k}}^2} = S\sqrt{J_{\mathbf{0}}^2 - J_{\mathbf{k}}^2}, \tag{10}$$

$$\Omega(k) = E_{\mathbf{k}}(\Sigma + \bar{\Sigma}) - B_{\mathbf{k}}(\Pi + \Pi^{\dagger}) - \omega(\Sigma - \bar{\Sigma}) - \Pi\Pi^{\dagger} + \Sigma\bar{\Sigma}, \tag{11}$$

$G(k) = \bar{G}(-k)$, $\Sigma(k) = \bar{\Sigma}(-k)$, and $\epsilon_{\mathbf{k}}^{(0)}$ is the spin-wave spectrum in the linear spin-wave approximation (classical spectrum). Quantity $\Omega(k)$ given by equation (11) describes renormalization of the spin-wave spectrum square. We find $\Omega(k)$ within the first three orders in $1/S$ in section 3 calculating the corresponding diagrams for the self-energy parts shown in figure 2.

It should be noted that we do not use the conventional Bogolyubov transformation in the technique described to diagonalize the bilinear part of the Hamiltonian (4). As a result anomalous Green's functions $F(k)$ and $F^{\dagger}(k)$ arise and momenta lie in the chemical BZ that is twice as large as the magnetic one. Such an approach proved to be more convenient as intermediate calculations turn out to be more compact while the final results are equivalent to those obtained using the conventional approach [16–20].

3. Spectrum renormalization

Although the spectrum renormalization within the first two orders in $1/S$ is well known, we present here the corresponding expressions for the sake of completeness.

3.1. First order in $1/S$

Only one diagram of the Hartree–Fock type shown in figure 2(a) contributes to the spectrum renormalization in the first order in $1/S$. The result can be represented in the form

$$\Sigma^{(a)}(k) = J_{\mathbf{0}}(A + B), \tag{12}$$

$$\Pi^{(a)}(k) = J_{\mathbf{k}}A, \tag{13}$$

$$\Pi^{\dagger(a)}(k) = J_{\mathbf{k}}(A + 2B), \tag{14}$$

$$\epsilon_{\mathbf{k}}^{(1)} = \epsilon_{\mathbf{k}}^{(0)}\left(1 + \frac{2(A+B)}{2S}\right) = \epsilon_{\mathbf{k}}^{(0)}\left(1 + \frac{0.158}{2S}\right), \tag{15}$$

where the following two constants are introduced:

$$A = \frac{1}{N}\sum_{\mathbf{k}} \frac{SJ_{\mathbf{k}}^2}{2J_0\epsilon_{\mathbf{k}}^{(0)}} \approx 0.2756, \tag{16}$$

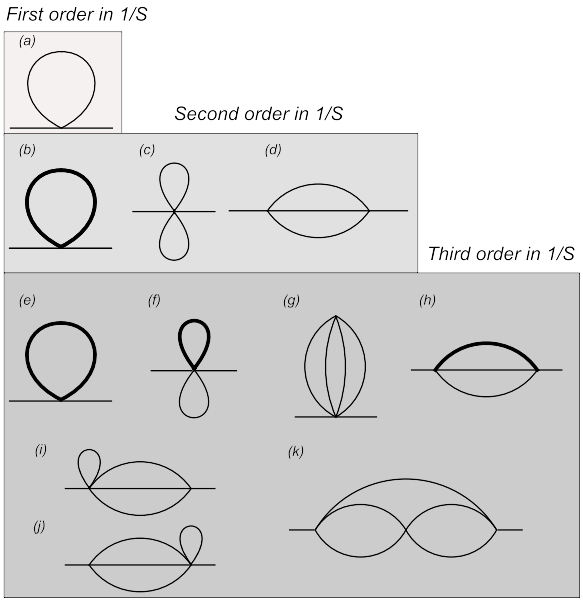

Figure 2. Diagrams contributing to the self-energy parts in the first three orders in $1/S$. Bold lines in diagrams (b), (f), and (h) denote Green's functions of the first order in $1/S$ (i.e. Green's functions given by equations (8) with self-energy parts calculated in the first order in $1/S$). The bold line in diagram (e) denotes Green's functions of the second order in $1/S$. Only diagrams (d) and (h)–(k) lead to the spectrum dispersion along the magnetic BZ boundary.

$$B = -\frac{1}{N}\sum_{\mathbf{k}} \frac{SJ_{\mathbf{0}} - \epsilon_{\mathbf{k}}^{(0)}}{2\epsilon_{\mathbf{k}}^{(0)}} \approx -0.1966. \tag{17}$$

It is seen from equation (15) that the renormalized spectrum remains flat on the BZ boundary in the first order in $1/S$ because $J_{\mathbf{k}} = 0$ for $|k_x| = \pi - |k_z|$. We draw $\epsilon_{\mathbf{k}}^{(1)}$ for $S = 1/2$ in figure 1 using equation (15).

3.2. Second order in $1/S$

Diagrams (b)–(d) shown in figure 2 contribute to self-energy parts in the second order in $1/S$. Diagram (b) is a schematic representation of the correction from diagram (a) of the second order in $1/S$ which arises after calculation of the diagram (a) with Green's functions of the first order in $1/S$ (i.e. Green's functions given by equations (8) with self-energy parts given by equations (12)–(14)).

3.2.1. Diagrams (b) and (c). It is convenient to group expressions for diagrams of the Hartree–Fock type (b) and (c) with the result

$$\Sigma^{(bc)}(k) = 0, \tag{18}$$

$$\Pi^{(bc)}(k) = J_{\mathbf{k}}\frac{A(A-2B)}{2S}, \tag{19}$$

$$\Pi^{\dagger(bc)}(k) = J_{\mathbf{k}}\frac{A^2 + B^2 + AB}{S}, \tag{20}$$

where A and B are given by equations (16) and (17), respectively. As $\Pi^{(bc)}(k)$, $\Pi^{\dagger(bc)}(k) \propto J_{\mathbf{k}}$, these diagrams do not contribute to the spectrum dispersion along the BZ boundary.

Table 1. Expressions are presented of the spin-wave spectrum $\epsilon_{\mathbf{k}}^{(3)}$ within the third order in $1/S$ at some representative points. Here $\epsilon_{\mathbf{k}}^{(0)}$ is the classical spectrum given by equation (10). The corresponding values of $\epsilon_{\mathbf{k}}^{(3)}$ are also shown for $S = 1/2$. Notice the smallness of the second-order $1/S$-corrections as compared with the first-order ones for all points and all S. In contrast, the absolute value of the third-order correction is approximately equal to the second-order one at $\mathbf{k} = (\pi, 0)$ for $S = 1/2$.

	$\epsilon_{\mathbf{k}}^{(3)}$	
k	Arbitrary S	$S = 1/2$
$\left(\frac{\pi}{4}, 0\right)$	$\epsilon_{\mathbf{k}}^{(0)}\left(1 + \frac{0.15795}{2S} + \frac{0.02476}{(2S)^2} - \frac{0.0033(3)}{(2S)^3}\right)$	1.2290(3)
$\left(\frac{\pi}{2}, 0\right)$	$\epsilon_{\mathbf{k}}^{(0)}\left(1 + \frac{0.15795}{2S} + \frac{0.02879}{(2S)^2} - \frac{0.0042(1)}{(2S)^3}\right)$	2.0482(2)
$\left(\frac{3\pi}{4}, 0\right)$	$\epsilon_{\mathbf{k}}^{(0)}\left(1 + \frac{0.15795}{2S} + \frac{0.02538}{(2S)^2} - \frac{0.0118(1)}{(2S)^3}\right)$	2.3179(2)
$(\pi, 0)$	$\epsilon_{\mathbf{k}}^{(0)}\left(1 + \frac{0.15795}{2S} + \frac{0.02134}{(2S)^2} - \frac{0.0172(1)}{(2S)^3}\right)$	2.3241(2)
$\left(\frac{3\pi}{4}, \frac{\pi}{4}\right)$	$\epsilon_{\mathbf{k}}^{(0)}\left(1 + \frac{0.15795}{2S} + \frac{0.02967}{(2S)^2} - \frac{0.0065(1)}{(2S)^3}\right)$	2.3622(2)
$\left(\frac{\pi}{2}, \frac{\pi}{2}\right)$	$\epsilon_{\mathbf{k}}^{(0)}\left(1 + \frac{0.15795}{2S} + \frac{0.03805}{(2S)^2} + \frac{0.0043(1)}{(2S)^3}\right)$	2.4007(2)
$\left(\frac{3\pi}{4}, \frac{3\pi}{4}\right)$	$\epsilon_{\mathbf{k}}^{(0)}\left(1 + \frac{0.15795}{2S} + \frac{0.02914}{(2S)^2} - \frac{0.0005(1)}{(2S)^3}\right)$	1.6781(2)

3.2.2. Diagram (d). One obtains for corrections to the self-energy parts from diagram (d)

$$\Sigma^{(\mathrm{d})}(k) = \frac{1}{N^2}\sum_{\mathbf{k}_1+\mathbf{k}_2+\mathbf{k}_3=\mathbf{k}} \frac{1}{4\epsilon_1\epsilon_2\epsilon_3(\omega^2-(\epsilon_1+\epsilon_2+\epsilon_3)^2)} \times ((SJ_0(\epsilon_1+\epsilon_2+\epsilon_3)-\omega\epsilon_1) \times (\tfrac{1}{2}S^2J_{\mathbf{k}}J_1J_2J_3 + S^2J_2^2J_3^2 - 2S^2J_0J_{1-\mathbf{k}}J_2J_3 + S^2J_2J_{2-\mathbf{k}}J_3J_{3-\mathbf{k}} + J_{1-\mathbf{k}}^2(S^2J_0^2-\epsilon_2\epsilon_3)) - (\epsilon_1+\epsilon_2+\epsilon_3)(S^3J_1J_2^2J_3J_{2-\mathbf{k}} + SJ_{\mathbf{k}}J_1J_{1-\mathbf{k}}(S^2J_0^2-\epsilon_2\epsilon_3))), \quad (21)$$

$$\Pi^{(\mathrm{d})}(k) = \frac{1}{N^2}\sum_{\mathbf{k}_1+\mathbf{k}_2+\mathbf{k}_3=\mathbf{k}} \frac{\epsilon_1+\epsilon_2+\epsilon_3}{4\epsilon_1\epsilon_2\epsilon_3(\omega^2-(\epsilon_1+\epsilon_2+\epsilon_3)^2)} \times (-\tfrac{1}{2}S^3J_1^3J_2J_3 + 2S^3J_0J_2J_{2-\mathbf{k}}J_3^2 - S^3J_1J_{2-\mathbf{k}}^2J_2J_3 - SJ_1J_{2-\mathbf{k}}J_{3-\mathbf{k}}(S^2J_0^2-\epsilon_2\epsilon_3)), \quad (22)$$

$$\Pi^{\dagger(\mathrm{d})}(k) = \frac{1}{N^2}\sum_{\mathbf{k}_1+\mathbf{k}_2+\mathbf{k}_3=\mathbf{k}} \frac{\epsilon_1+\epsilon_2+\epsilon_3}{4\epsilon_1\epsilon_2\epsilon_3(\omega^2-(\epsilon_1+\epsilon_2+\epsilon_3)^2)} \times (-\tfrac{1}{2}S^3J_{\mathbf{k}}^2J_1J_2J_3 + 2S^3J_0J_{\mathbf{k}}J_1J_{2-\mathbf{k}}J_3 - S^3J_1^3J_2J_3 + 2S^3J_0J_1J_{1-\mathbf{k}}J_2^2 - S^3J_{1-\mathbf{k}}^2J_1J_2J_3 - (2SJ_{\mathbf{k}}J_1^2 + SJ_1J_2J_3 + 2SJ_0J_1J_{1-\mathbf{k}} + SJ_1J_{2-\mathbf{k}}J_{3-\mathbf{k}})(S^2J_0^2-\epsilon_2\epsilon_3)), \quad (23)$$

where we drop the superscript (0) in $\epsilon_{1,2,3}^{(0)}$ to simplify the notation. Sums in equations (21)–(23) over each momentum were calculated numerically by summing up L^2 points in the BZ with some particular values of L ranging from 20 to 200 and extrapolating the results to $L = \infty$ using the formula $A_\infty + A_1/L + A_2/L^2 + \cdots$, as done in previous papers [15, 7, 8]. Appropriate symmetry of the summands was also used.

In accordance with previous results [7, 8] we obtain that this diagram leads to a very small difference of 1.4% between $\epsilon_{(\pi,0)}^{(2)} \approx 2.35858$ and $\epsilon_{(\pi/2,\pi/2)}^{(2)} \approx 2.39199$. It is seen from table 1 that the second-order corrections are much smaller than the first-order ones in the whole BZ for all S. The spectrum $\epsilon_{\mathbf{k}}^{(2)}$ is presented in figure 1 for $S = 1/2$.

3.3. Third order in $1/S$

One has to analyze in this order the diagrams shown in figures 2(e)–(k). Diagram (e) represents the second-order correction from diagram (a) which should be calculated using equations (12)–(23). Bold lines in diagrams (f) and (h) denote Green's functions of the first order in $1/S$. Expressions for the self-energy parts in this order are quite complicated and the reader is referred to the appendix for some detail of the calculations. It can be shown (see appendix) that diagrams of the Hartree–Fock type presented in figures 2(e)–(g) do not change along the BZ boundary so that only diagrams (h)–(k) give rise to the spectrum dispersion in these directions in this order. In contrast to the second-order corrections (21)–(23) one has to calculate triple sums over momenta in the third order; this procedure requires much computer time. Then, we focus on short-wavelength magnons as their spectrum renormalization is expected to be most pronounced and calculate $\epsilon_{\mathbf{k}}^{(3)}$ in a number of points with $|\mathbf{k}|, |\mathbf{k}-\mathbf{k}_0| \geqslant \pi/8$. The results are presented in figure 1 (for $S = 1/2$) and in table 1.

It is seen from table 1 that the third-order corrections are noticeable only for $S \sim 1$ and only in the vicinity of the point $\mathbf{k} = (\pi, 0)$. In particular, absolute values of the third-and the second-order corrections in $1/S$ are approximately equal to each other at $\mathbf{k} = (\pi, 0)$ for $S = 1/2$. The excitation energy in a spin-$\frac{1}{2}$ 2D AF $\epsilon_{(\pi,0)}^{(3)} \approx 2.3241(2)$ is 3.2% smaller than $\epsilon_{(\pi/2,\pi/2)}^{(3)} \approx 2.4007(2)$ which improves the agreement with the recent experiments and numerical results leaving it, however, far from being perfect. Thus, our calculations demonstrate that quantum renormalization of the spectrum near $\mathbf{k} = (\pi, 0)$ for $S = 1/2$ is described by a slowly converging $1/S$ series.

It is also seen from table 1 that at $\mathbf{k} = (\pi, 0)$ the third-order correction is only 2.5 times smaller than the second-order one for $S = 1$. Thus, one can expect a slow convergence of the $1/S$ series near $\mathbf{k} = (\pi, 0)$ also for $S = 1$. Meantime the overall renormalization of the spectrum would be small due to very small values of high-order $1/S$ terms.

4. Conclusion

To conclude, we calculate the spin-wave spectrum of a 2D AF on a square lattice in the third order in $1/S$ to examine the convergence of the $1/S$ series. Within the first two orders we recover the previous results [7, 8] showing that the second-order corrections are much smaller than the first-order ones in the whole BZ and for all S (see table 1). Our calculation of the spectrum in the next order demonstrates that the third-order corrections to the spectrum are much smaller than the second-order ones in the whole BZ except in the vicinity of the point $\mathbf{k} = (\pi, 0)$ in the case of $S \sim 1$. In particular, their absolute values are approximately equal at $\mathbf{k} = (\pi, 0)$ for $S = 1/2$ (see table 1 and figure 1). Thus, our results demonstrate that, unlike other quantities, quantum

renormalization of the spectrum near $\mathbf{k} = (\pi, 0)$ for $S \sim 1$ is described by a slowly converging $1/S$ series. We find that third-order corrections for the spectrum improve the agreement with the recent experiments and numerical results in a spin-$\frac{1}{2}$ 2D AF. We expect slow convergence of the $1/S$ series near $\mathbf{k} = (\pi, 0)$ also for $S = 1$, while the overall renormalization of the spectrum would be small in this case due to the very small values of high-order $1/S$ corrections.

Acknowledgments

This work was supported by the President of the Russian Federation (grant MK-329.2010.2), RFBR grants 09-02-00229, and Russian Programs 'Quantum Macrophysics', 'Strongly correlated electrons in semiconductors, metals, superconductors and magnetic materials', and 'Neutron Research of Solids'.

Appendix. Expressions for the third-order diagrams

We present in this appendix expressions for self-energy parts in the third order in $1/S$ which originate from the diagrams shown in figures 2(e)–(k). Simple codes have been written in Mathematica software to generate the majority of these expressions. To make it compact, we present below an expression for the sum of anomalous self-energy parts $\Pi(k) + \Pi^{\dagger}(k)$ rather than for $\Pi(k)$ and $\Pi^{\dagger}(k)$ separately because only this sum contributes to the spectrum renormalization in this order (see equation (11)).

A.1. Diagrams (e) and (f)

It is convenient to group contributions from diagrams of the Hartree–Fock type shown in figures 2(e) and (f). One has after simple calculations using expressions (12)–(23)

$$\begin{aligned}\Sigma^{(\mathrm{ef})}(k) &= -J_0\frac{A^3}{(2S)^2}\\ &+ \frac{1}{N^3}\sum_{\mathbf{k}_1+\mathbf{k}_2+\mathbf{k}_3+\mathbf{k}_4=0}\frac{S}{32\epsilon_1\epsilon_2\epsilon_3\epsilon_4(\epsilon_1+\epsilon_2+\epsilon_3+\epsilon_4)^2}\\ &\times(-3S^2J_1^3J_2J_3J_4\epsilon_1 + J_1J_4(-15S^2J_2^3J_3\epsilon_1\\ &+ 8S^2J_0J_2^2J_{1+4}\epsilon_4 + 8S^2J_0J_3J_4J_{2+4}(\epsilon_1+\epsilon_4)\\ &+ 2J_2J_3(3\epsilon_1\epsilon_2\epsilon_3 - S^2(3J_0^2+2J_{1+4}^2)\epsilon_4))\\ &+ 4(J_4^2J_{1+4}^2\epsilon_1(-S^2J_0^2+\epsilon_2\epsilon_3) - 3J_2^2J_4^2(S^2J_3^2\epsilon_1\\ &+ \epsilon_2(S^2J_0^2-\epsilon_1\epsilon_3)) + J_2(4S^2J_0^3J_4J_{2+4}\epsilon_2\\ &+ 2J_0J_4\epsilon_1(S^2J_3(2J_4J_{1+4}+J_3J_{2+4}) - 2J_{2+4}\epsilon_2\epsilon_3)\\ &+ S^2J_0^2J_{3+4}(J_3J_{2+4}(\epsilon_1-\epsilon_4) - J_4J_{1+4}\epsilon_4)\\ &+ J_4J_{3+4}\epsilon_1(-S^2J_3J_4J_{2+4} + J_{1+4}\epsilon_3\epsilon_4)))), \qquad (A.1)\end{aligned}$$

$$\begin{aligned}\Pi^{(\mathrm{ef})}(k) + \Pi^{\dagger(\mathrm{ef})}(k) &= J_{\mathbf{k}}\frac{A(B^2+(B-A)^2)}{2S^2}\\ &+ 2\frac{J_{\mathbf{k}}}{J_0}\Sigma^{(\mathrm{ef})}(k) + \frac{J_{\mathbf{k}}}{J_0}\frac{1}{8N^3}\\ &\times\sum_{\mathbf{k}_1+\mathbf{k}_2+\mathbf{k}_3+\mathbf{k}_4=0}\frac{1}{\epsilon_1\epsilon_2\epsilon_3\epsilon_4(\epsilon_1+\epsilon_2+\epsilon_3+\epsilon_4)}\\ &\times(SJ_3J_4(S^2J_1^3J_2 - 2S^2J_0J_1J_{2+4}J_4\\ &+ (J_1J_2 - 2J_0J_{3+4} + 2J_3J_4)(S^2J_0^2-\epsilon_1\epsilon_2))), \qquad (A.2)\end{aligned}$$

where A and B are given by equations (16) and (17), respectively. Sums in equations (A.1) and (A.2) were calculated as described above in section 3.2.2 for diagram (d) with $20 \leqslant L \leqslant 96$. These sums arise after taking into account in the Green's functions involved in diagram (e) contributions to self-energy parts from diagram (d). We obtain numerically from equations (A.1) and (A.2) $\Sigma^{(\mathrm{ef})}(k) = \frac{0.0598(2)}{(2S)^2}$ and $\Pi^{(\mathrm{ef})}(k) + \Pi^{\dagger(\mathrm{ef})}(k) = J_{\mathbf{k}}\frac{0.1446(1)}{(2S)^2}$.

A.2. Diagram (g)

Corrections to self-energy parts from another Hartree–Fock diagram shown in figure 2(g) have the form

$$\begin{aligned}\Sigma^{(\mathrm{g})}(k) &= \frac{1}{16N^3}\sum_{\mathbf{k}_1+\mathbf{k}_2+\mathbf{k}_3+\mathbf{k}_4=0}\frac{1}{\epsilon_1\epsilon_2\epsilon_3\epsilon_4(\epsilon_1+\epsilon_2+\epsilon_3+\epsilon_4)}\\ &\times(SJ_3J_4(S^2J_1^3J_2 - 2S^2J_0J_1J_{2+4}J_4\\ &+ (J_1J_2 - 2J_0J_{3+4} + 2J_3J_4)(S^2J_0^2-\epsilon_1\epsilon_2))), \qquad (A.3)\end{aligned}$$

$$\begin{aligned}\Pi^{(\mathrm{g})}(k) + \Pi^{\dagger(\mathrm{g})}(k) &= \frac{J_{\mathbf{k}}}{J_0}\frac{1}{N^3}\\ &\times\sum_{\mathbf{k}_1+\mathbf{k}_2+\mathbf{k}_3+\mathbf{k}_4=0}\frac{1}{8S\epsilon_1\epsilon_2\epsilon_3\epsilon_4(\epsilon_1+\epsilon_2+\epsilon_3+\epsilon_4)}\\ &\times J_{1+2}(S^2(-2S^2J_0^3J_1J_2 + S^2J_0^4J_{1+2}\\ &- 3S^2J_0J_1^2J_3J_4 + J_0^2(S^2J_{1+3}(2J_2J_3+J_1J_4)\\ &- 2J_{1+2}\epsilon_1\epsilon_2) + J_1J_4(S^2J_2J_{1+2}J_3 + J_{1+3}\epsilon_2\epsilon_3))\\ &+ (J_{1+2}\epsilon_1\epsilon_2\epsilon_3 + 2S^2J_2(-J_3J_{1+3}\epsilon_1 + J_0J_1\epsilon_3))\epsilon_4). \qquad (A.4)\end{aligned}$$

Notice the identity of sums in equations (A.3) and (A.2). Sums in equations (A.3) and (A.4) were calculated with $20 \leqslant L \leqslant 96$. We obtain numerically from equations (A.3) and (A.4) $\Sigma^{(\mathrm{g})}(k) = -\frac{0.058\,92(2)}{(2S)^2}$ and $\Pi^{(\mathrm{g})}(k) + \Pi^{\dagger(\mathrm{g})}(k) = -J_{\mathbf{k}}\frac{0.028\,00(4)}{(2S)^2}$.

A.3. Diagram (h)

It is convenient to divide the corrections from the diagram shown in figure 2(h) into two parts: $\Sigma^{(\mathrm{h})}(k) = \Sigma_1^{(\mathrm{h})}(k) + \Sigma_2^{(\mathrm{h})}(k)$, $\Pi^{(\mathrm{h})}(k) = \Pi_1^{(\mathrm{h})}(k) + \Pi_2^{(\mathrm{h})}(k)$, and $\Pi^{\dagger(\mathrm{h})}(k) = \Pi_1^{\dagger(\mathrm{h})}(k) + \Pi_2^{\dagger(\mathrm{h})}(k)$, where the first terms arise after taking into account first-order $1/S$ corrections to self-energy parts in the numerators of Green's functions in diagram (d). As a result one has for them

$$\begin{aligned}\Sigma_1^{(\mathrm{h})}(k) &= \frac{1}{N^2}\sum_{\mathbf{k}_1+\mathbf{k}_2+\mathbf{k}_3=\mathbf{k}}\frac{1}{4\epsilon_1\epsilon_2\epsilon_3(\omega^2-(\epsilon_1+\epsilon_2+\epsilon_3)^2)}\\ &\times((\epsilon_1+\epsilon_2+\epsilon_3)(\tfrac{1}{2}(3A+B)S^2J_0J_{\mathbf{k}}J_1J_2J_3\\ &- (3A+2B)S^2J_0^2J_{1-\mathbf{k}}(J_{\mathbf{k}}J_1+2J_2J_3)\\ &+ AJ_{\mathbf{k}}J_1J_{1-\mathbf{k}}\epsilon_2\epsilon_3 + (3A+B)S^2J_0J_2^2J_3^2\\ &- (3A+2B)S^2J_1^2J_{1-\mathbf{k}}J_2J_3\\ &+ 3(A+B)S^2J_0J_2J_{2-\mathbf{k}}J_3J_{3-\mathbf{k}} + 3(A+B)S^2J_0^3J_{1-\mathbf{k}}^2\\ &- (A+B)J_0J_{1-\mathbf{k}}^2\epsilon_2\epsilon_3) - \omega\epsilon_1(2ASJ_2^2J_3^2\\ &- (2A+B)2SJ_0J_{1-\mathbf{k}}J_2J_3 + 2S(A+B)\\ &\times(J_2J_{2-\mathbf{k}}J_3J_{3-\mathbf{k}} + J_0^2J_{1-\mathbf{k}}^2) + ASJ_{\mathbf{k}}J_1J_2J_3)), \qquad (A.5)\end{aligned}$$

$$\Pi_1^{(\mathrm{h})}(k)+\Pi_1^{\dagger(\mathrm{h})}(k)=\frac{1}{N^2}$$
$$\times\sum_{\mathbf{k}_1+\mathbf{k}_2+\mathbf{k}_3=\mathbf{k}}\frac{\epsilon_1+\epsilon_2+\epsilon_3}{4\epsilon_1\epsilon_2\epsilon_3(\omega^2-(\epsilon_1+\epsilon_2+\epsilon_3)^2)}$$
$$\times(6(A+B)S^2J_0^3J_2J_{2-\mathbf{k}}$$
$$-S^2J_0^2(J_3((3A+2B)J_1J_2+6(A+B)J_{1-\mathbf{k}}J_{2-\mathbf{k}})$$
$$+2(3A+2B)J_1^2J_{\mathbf{k}})+\tfrac{1}{2}J_3(-S^2J_1J_2((9A+4B)J_1^2$$
$$+12(A+B)J_{3-\mathbf{k}}^2+(3A+2B)J_{\mathbf{k}}^2)$$
$$+2(AJ_1J_2+2(A+B)J_{1-\mathbf{k}}J_{2-\mathbf{k}}+2AJ_3J_{\mathbf{k}})\epsilon_1\epsilon_2)$$
$$+2J_0(2(3A+2B)S^2J_1^2J_2J_{2-\mathbf{k}}$$
$$+(A+B)J_3(3S^2J_2J_{1-\mathbf{k}}J_{\mathbf{k}}-J_{3-\mathbf{k}}\epsilon_1\epsilon_2))). \quad (A.6)$$

Expressions for $\Sigma_2^{(\mathrm{h})}(k)$, $\Pi_2^{(\mathrm{h})}(k)$, and $\Pi_2^{\dagger(\mathrm{h})}(k)$ can be easily obtained from equations (21)–(23) taking into account the first-order renormalization of the spectrum $\epsilon_{\mathbf{k}}^{(1)}=\epsilon_{\mathbf{k}}^{(0)}(1+(A+B)/S)$ and the fact that one has to put $\epsilon_{\mathbf{k}}^{(1)}$ instead of ω calculating the third-order correction to the spectrum. Sums in equations (A.5) and (A.6) were calculated with $20\leqslant L\leqslant 200$.

A.4. Diagrams (i) and (j)

Grouping expressions for diagrams shown in figures 2(i) and (j) one obtains

$$\Sigma^{(\mathrm{ij})}(k)=\frac{1}{N^2}\sum_{\mathbf{k}_1+\mathbf{k}_2+\mathbf{k}_3=\mathbf{k}}\frac{1}{4\epsilon_1\epsilon_2\epsilon_3(\omega^2-(\epsilon_1+\epsilon_2+\epsilon_3)^2)}$$
$$\times((SJ_0(\epsilon_1+\epsilon_2+\epsilon_3)-\omega\epsilon_1)$$
$$\times\Big(BSJ_{\mathbf{k}}J_1J_2J_3+2BSJ_2^2J_3^2-2(A+B)SJ_0J_{1-\mathbf{k}}J_2J_3$$
$$+2ASJ_2J_{2-\mathbf{k}}J_3J_{3-\mathbf{k}}+\frac{2}{S}AJ_{1-\mathbf{k}}^2(S^2J_0^2-\epsilon_2\epsilon_3)\Big)$$
$$+2ASJ_2J_{2-\mathbf{k}}J_3J_{3-\mathbf{k}}(SJ_0(\epsilon_1+\epsilon_2+\epsilon_3)+\omega\epsilon_1)$$
$$-(\epsilon_1+\epsilon_2+\epsilon_3)(\tfrac{1}{2}(3A+2B)S^2J_1J_2^2J_3J_{2-\mathbf{k}}$$
$$+(A+B)J_{\mathbf{k}}J_1J_{1-\mathbf{k}}(S^2J_0^2-\epsilon_2\epsilon_3))), \quad (A.7)$$
$$\Pi^{(\mathrm{ij})}(k)+\Pi^{\dagger(\mathrm{ij})}(k)=\frac{1}{N^2}$$
$$\times\sum_{\mathbf{k}_1+\mathbf{k}_2+\mathbf{k}_3=\mathbf{k}}\frac{\epsilon_1+\epsilon_2+\epsilon_3}{4\epsilon_1\epsilon_2\epsilon_3(\omega^2-(\epsilon_1+\epsilon_2+\epsilon_3)^2)}$$
$$\times(-BS^2J_{\mathbf{k}}^2J_1J_2J_3+(3A+2B)S^2J_0J_{\mathbf{k}}J_1J_{2-\mathbf{k}}J_3$$
$$-3BS^2J_1^3J_2J_3+2(3A+2B)S^2J_0J_1J_{1-\mathbf{k}}J_2^2$$
$$-4AS^2J_{1-\mathbf{k}}^2J_1J_2J_3-4AS^2J_0^2J_{1-\mathbf{k}}J_{2-\mathbf{k}}J_3$$
$$-(4BJ_{\mathbf{k}}J_1^2+2BJ_1J_2J_3-2(A+B)J_0J_1J_{1-\mathbf{k}}$$
$$+2AJ_1J_{2-\mathbf{k}}J_{3-\mathbf{k}})(S^2J_0^2-\epsilon_2\epsilon_3)). \quad (A.8)$$

Sums in equations (A.7) and (A.8) were calculated with $20\leqslant L\leqslant 200$.

A.5. Diagram (k)

Expressions stemming from this diagram are very cumbersome. We present here only an expression for $\Sigma^{(\mathrm{k})}(k)$ in the most compact form (i.e. before integration over energies) for the particular case of the momentum $\mathbf{k}$ lying on the BZ boundary (i.e. for $|k_x|=\pi-|k_z|$ and $J_{\mathbf{k}}=0$) that has the form

$$\Sigma^{(\mathrm{k})}(k)=-\mathrm{i}\frac{1}{N^3}\sum(-8F_1G_5\bar{G}_2\bar{G}_3\bar{G}_4J_{1-\mathbf{k}}J_2J_{2-\mathbf{k}}$$
$$-8F_4G_1G_3\bar{G}_2\bar{G}_5J_1J_{1-\mathbf{k}}J_{4-\mathbf{k}}-8F_4F_5G_1G_3\bar{G}_2J_1J_4J_{4-\mathbf{k}}$$
$$-8F_2G_3G_5\bar{G}_1\bar{G}_4(2J_{1-\mathbf{k}}^2J_2+J_{2-\mathbf{k}}J_4J_{4-\mathbf{k}})$$
$$-8F_1F_2F_5G_3G_4J_1J_{1-\mathbf{k}}J_{2+4}$$
$$-8F_5G_2G_3G_4\bar{G}_1J_{1-\mathbf{k}}J_2J_{2+4}$$
$$-8F_3\bar{G}_1\bar{G}_2\bar{G}_4\bar{G}_5J_{1-\mathbf{k}}J_4J_{2+4}-8F_4F_5G_2G_3\bar{G}_1J_3J_4J_{2+4}$$
$$-8F_2F_3\bar{G}_1\bar{G}_4\bar{G}_5J_3J_4J_{2+4}-8F_1\bar{G}_2\bar{G}_3\bar{G}_4\bar{G}_5J_{3-\mathbf{k}}J_4J_{2+4}$$
$$-8F_2F_4F_5G_1G_3J_1J_{4-\mathbf{k}}J_{2+4}-8F_1F_4F_5G_2G_3J_2J_{4-\mathbf{k}}J_{2+4}$$
$$-8G_3G_5\bar{G}_1\bar{G}_2\bar{G}_4J_{2-\mathbf{k}}J_{4-\mathbf{k}}J_{2+4}$$
$$-8G_1\bar{G}_2\bar{G}_3\bar{G}_4\bar{G}_5J_{2-\mathbf{k}}J_{4-\mathbf{k}}J_{2+4}$$
$$-8F_1F_4F_5\bar{G}_2\bar{G}_3J_{2-\mathbf{k}}(J_{1-\mathbf{k}}J_3+J_4J_{2+4})$$
$$-8F_1G_3G_5\bar{G}_2\bar{G}_4(J_1J_{1-\mathbf{k}}^2+J_3J_{4-\mathbf{k}}J_{2+4})$$
$$-4F_1F_2F_3F_4F_5(J_1(2J_{1-\mathbf{k}}^2+3J_2^2)$$
$$+2J_4(J_{1-\mathbf{k}}J_{4-\mathbf{k}}+2J_{3-\mathbf{k}}J_{2+4}))$$
$$-4F_2F_3F_4F_5\bar{G}_1(4J_{1-\mathbf{k}}J_2J_3+J_{2-\mathbf{k}}(J_1J_3+2J_{4-\mathbf{k}}J_{2+4}))$$
$$-8F_2F_5G_3G_4\bar{G}_1J_{1-\mathbf{k}}(2J_2J_4+J_{1-\mathbf{k}}J_{3+4})$$
$$-4F_4F_5G_3\bar{G}_1\bar{G}_2(4J_{1-\mathbf{k}}(J_{1-\mathbf{k}}^2+J_4^2)$$
$$+J_{2-\mathbf{k}}(J_1J_2+4J_{4-\mathbf{k}}J_{3+4}))$$
$$-8F_2F_3F_4F_5G_1J_{4-\mathbf{k}}(J_{2-\mathbf{k}}J_{2+4}+J_1J_5)$$
$$-8F_2F_5G_3\bar{G}_1\bar{G}_4J_{1-\mathbf{k}}(J_2J_4+J_3J_5)$$
$$-16F_1F_3F_5G_4\bar{G}_2J_{1-\mathbf{k}}(J_{2-\mathbf{k}}J_4+J_{3-\mathbf{k}}J_5)$$
$$-8F_2F_5\bar{G}_1\bar{G}_3\bar{G}_4(2J_{1-\mathbf{k}}J_2J_4+J_{1-\mathbf{k}}^2J_{3+4}+J_1J_{3-\mathbf{k}}J_5)$$
$$-8F_3F_4F_5\bar{G}_1\bar{G}_2(2J_{1-\mathbf{k}}^2J_2+J_2J_4^2+J_{1-\mathbf{k}}J_4J_{3+4}$$
$$+J_{4-\mathbf{k}}(J_{2-\mathbf{k}}J_4+J_1J_{3+4})+J_3J_4J_5)$$
$$-8F_3F_4F_5G_2\bar{G}_1(2J_{1-\mathbf{k}}^2J_2+J_2J_4^2$$
$$+J_{1-\mathbf{k}}J_4J_{3+4}+(J_3J_4+J_{3-\mathbf{k}}J_{4-\mathbf{k}})J_5)$$
$$-8F_1F_3F_5\bar{G}_2\bar{G}_4(J_1(J_2J_4+J_{1-\mathbf{k}}J_{3+4}+2J_3J_5)$$
$$+2J_{1-\mathbf{k}}(J_{2-\mathbf{k}}J_4+J_{3-\mathbf{k}}J_5))$$
$$-8F_2G_5\bar{G}_1\bar{G}_3\bar{G}_4(2J_{1-\mathbf{k}}^2J_2+J_{4-\mathbf{k}}(J_1J_{3+4}+J_{3-\mathbf{k}}J_5))$$
$$-8F_1F_2F_4F_5\bar{G}_3(2J_{1-\mathbf{k}}^2J_{2-\mathbf{k}}+J_1(2J_{1-\mathbf{k}}J_2+J_4J_{3+4})$$
$$+J_4(2J_{2-\mathbf{k}}J_4+J_2J_{4-\mathbf{k}}+2J_{3-\mathbf{k}}J_5))$$
$$-4F_1F_4F_5G_3\bar{G}_2(2J_{2-\mathbf{k}}J_4J_{2+4}$$
$$+2J_{4-\mathbf{k}}(J_3J_{3+4}+J_{1-\mathbf{k}}J_5)+J_1(J_2J_3+2J_4J_5))$$
$$-8F_2F_5G_1\bar{G}_3\bar{G}_4((J_1J_2+2J_{1-\mathbf{k}}J_{2-\mathbf{k}})J_{4-\mathbf{k}}+J_1J_3J_{5-\mathbf{k}})$$
$$-8F_1F_5G_3G_4\bar{G}_2(J_1J_{1-\mathbf{k}}J_4+J_2J_3J_{5-\mathbf{k}})$$
$$-8F_2F_3F_5G_1\bar{G}_4(J_1J_{1-\mathbf{k}}J_{4-\mathbf{k}}+J_{2-\mathbf{k}}(J_2J_{4-\mathbf{k}}+J_3J_{5-\mathbf{k}}))$$
$$-8F_4G_1\bar{G}_2\bar{G}_3\bar{G}_5J_{2-\mathbf{k}}(J_2J_{4-\mathbf{k}}+J_3J_{5-\mathbf{k}}+J_1J_{2+5})$$
$$-8F_1F_5\bar{G}_2\bar{G}_3\bar{G}_4(J_{2-\mathbf{k}}(J_2J_4+J_3J_5)$$
$$+(J_1J_2+2J_{1-\mathbf{k}}J_{2-\mathbf{k}})J_{2+5})$$
$$-8F_1F_2F_3F_4G_5(J_2J_{2-\mathbf{k}}J_4+J_2^2J_{4-\mathbf{k}}$$
$$+J_{2-\mathbf{k}}(J_3J_5+2J_{1-\mathbf{k}}J_{2+5})+J_1(J_{1-\mathbf{k}}J_4+J_2J_{2+5}))$$
$$-8F_1F_3G_5\bar{G}_2\bar{G}_4(2J_{1-\mathbf{k}}^2J_{2-\mathbf{k}}+J_3J_{4-\mathbf{k}}J_5$$
$$+J_1(2J_{1-\mathbf{k}}J_2+J_5J_{3+5}))), \quad (A.9)$$

where the momentum conservation laws $k_1+k_2+k_3=k_1+k_4+k_5=k$ are implied. The expression for $\Sigma^{(\mathrm{k})}(k)$

for arbitrary momentum and those for anomalous self-energy parts are much more cumbersome than equation (A.9) and we do not present them here. Corresponding sums over momenta were calculated with $16 \leqslant L \leqslant 64$.

References

[1] Manousakis E 1991 The spin-1/2 Heisenberg antiferromagnet on a square lattice and its application to the cuprous oxides *Rev. Mod. Phys.* **63** 1–62

[2] Chakravarty S, Halperin B I and Nelson D R 1989 Two-dimensional quantum Heisenberg antiferromagnet at low temperatures *Phys. Rev.* B **39** 2344–71

[3] Christensen N B, Ronnow H M, McMorrow D F, Harrison A, Perring T G, Enderle M, Coldea R, Regnault L P and Aeppli G 2007 *Proc. Natl Acad. Sci. USA* **104** 15264

[4] Kim Y J, Aharony A, Birgeneau R J, Chou F C, Entin-Wohlman O, Erwin R W, Greven M, Harris A B, Kastner M A, Korenblit I Ya, Lee Y S and Shirane G 1999 Ordering due to quantum fluctuations in $Sr_2Cu_3O_4Cl_2$ *Phys. Rev. Lett.* **83** 852–5

[5] Rønnow H M, McMorrow D F, Coldea R, Harrison A, Youngson I D, Perring T G, Aeppli G, Syljuåsen O, Lefmann K and Rischel C 2001 Spin dynamics of the 2d spin 12 quantum antiferromagnet copper deuteroformate tetradeuterate (cftd) *Phys. Rev. Lett.* **87** 037202

[6] Lumsden M D, Nagler S E, Sales B C, Tennant D A, McMorrow D F, Lee S-H and Park S 2006 Magnetic excitation spectrum of the square lattice $s = 1/2$ Heisenberg antiferromagnet $K_2V_3O_8$ *Phys. Rev.* B **74** 214424

[7] Igarashi J and Nagao T 2005 *Phys. Rev.* B **72** 014403

[8] Igarashi J 1992 1/s expansion for thermodynamic quantities in a two-dimensional Heisenberg antiferromagnet at zero temperature *Phys. Rev.* B **46** 10763–71

[9] Hsu T C 1990 *Phys. Rev.* B **41** 11379

[10] Zheng W, Oitmaa J and Hamer C J 2005 *Phys. Rev.* B **71** 184440

[11] Sandvik A W and Singh R R P 2001 *Phys. Rev. Lett.* **86** 528

[12] Hamer C J, Zheng W and Arndt P 1992 *Phys. Rev.* B **46** 6276

[13] Hamer C J, Zheng W and Oitmaa J 1994 *Phys. Rev.* B **50** 6877

[14] Igarashi J and Watabe A 1991 Quantum corrections to the spin-correlation function and the spin-stiffness constant in a two-dimensional Heisenberg antiferromagnet at zero temperature *Phys. Rev.* B **44** 5057–63

[15] Zheng W and Hamer C J 1993 *Phys. Rev.* B **47** 7961

[16] Petitgrand D, Maleyev S V, Bourges Ph and Ivanov A S 1999 Pseudodipolar interaction and antiferromagnetism in R_2CuO_4 compounds (R = Pr, Nd, Sm, and Eu) *Phys. Rev.* B **59** 1079–104

[17] Maleyev S V 2000 Spin-wave interaction and renormalization of magnetic anisotropy in 2d antiferromagnets *Phys. Rev. Lett.* **85** 3281–4

[18] Syromyatnikov A V and Maleyev S V 2001 Spin-wave interaction in two- and three-dimensional antiferromagnets in a weak magnetic field *Phys. Rev.* B **65** 012401

[19] Ohyama T and Shiba H 1994 Spin dynamics and quantum fluctuations in quasi-one-dimensional triangular antiferromagnets: magnetic field effects *J. Phys. Soc. Japan* **63** 3454–73

[20] Ohyama T and Shiba H 1993 Nonlinear excitations in quasi-one-dimensional triangular antiferromagnets *J. Phys. Soc. Japan* **62** 3277–93